



## Article

# Potential and limitations of satellite altimetry constellations for monitoring surface water storage changes – A case study in the Mississippi basin

Denise Dettmering <sup>1,\*</sup> , Laura Ellenbeck <sup>1</sup>, Daniel Scherer <sup>1</sup> , Christian Schwatke <sup>1</sup> and Christoph Niemann <sup>2</sup>

<sup>1</sup> Deutsches Geodätisches Forschungsinstitut der Technischen Universität München (DGFI-TUM), Germany

<sup>2</sup> Goethe Universität, Frankfurt am Main, Germany

\* Correspondence: denise.dettmering@tum.de

Version August 25, 2020 submitted to Remote Sens.

**Abstract:** Remote sensing data are essential for monitoring Earth's surface waters, especially since the number of publicly available in-situ data is declining. Satellite altimetry provides valuable information on water level and its variations for lakes, reservoirs, and rivers. In combination with satellite imagery, the derived time series allow for monitoring lake storage changes and river discharge. However, satellite altimetry is limited in spatial resolution due to its measurement geometry, only providing information in nadir direction beneath the satellite's orbit. In a case study in the Mississippi River Basin (MRB), this study investigates the potential and the limitations of past and current satellite missions to monitor basin-wide storage changes. For that purpose an automated target detection is developed and the extracted lake surfaces are merged with the satellites' tracks. This reveals that the current altimeter configuration misses about 80% of all lakes larger than  $0.1 \text{ km}^2$  in the MRB, and still 20% of lakes larger than  $10 \text{ km}^2$ , corresponding to 30% and 7% of surface area, respectively. Past altimetry configurations perform even worse. From the water bodies represented by a global hydrology model, at least 91% of targets and 98% of storage changes are captured by the current altimeter configuration. This will significantly improve with the launch of the planned SWOT mission.

**Keywords:** satellite altimetry; terrestrial water storage; Mississippi basin; SWOT

## 1. Introduction

Freshwater resources are critical for human life. Only about 2.5% of the Earth's water is freshwater, from which most is embedded in ice and in the ground [1]. About 0.25% of the World's freshwater is stored in lakes and reservoirs. The knowledge about its availability and changes is essential for water management as well as for monitoring climate change. Even though, today, for some regions extensive and precise in-situ monitoring systems has been installed, the knowledge about global water storage is still limited. Global models such as the WaterGap Global Hydrology Model WGHM [2] can provide valuable but uncertain information. In order to provide reliable results they need to be calibrated by observation data [3].

During the last years, the availability of public in-situ data has been steadily decreasing. In the same time, remote sensing techniques allow for the monitoring of surface waters on a global scale and without the need of any infrastructure on ground. Even if the quality of the satellite data is normally not as good as ground-based measurements, it is a valuable data source, especially in remote areas [4]. Surface volume changes can be measured by satellites with two different approaches: Whereas gravity missions such as the Gravity Recovery and Climate Experiment (GRACE) and its successor

GRACE-FO observe total water storage changes with spatial resolutions of some hundred kilometres [5], a combination of satellite altimetry and optical imagery can be used to directly estimate surface water volume changes [6–8].

In contrast to GRACE and satellite imagery, due to its measurement principle, satellite altimetry only deliver data along the satellites' ground tracks, i.e. so-called along-track data directly beneath the satellites. Depending on the active missions and its orbit configurations some lakes are missed for which no height information can be derived. The focus of this study is to investigate the capability of different satellite altimetry configurations to measure basin-wide lake storage changes. As study case, the Mississippi basin in North America is used. In order to allow for a comprehensive inventory of lakes and reservoirs covered by different satellite altimetry missions, an automatic tool for lake detection has been developed as part of the study. Model storage information from WGHM is used to assess the percentage of water volume changes missed due to the current insufficient data coverage of satellite altimetry as well as the improvements expected from the upcoming new SWOT mission [9].

The paper is structured as follow. Section 2 describes the study area and the used input data sets. Afterwards, Sect. 3 introduced the used methods before Sect. 4 presents the results of the study followed by a discussion in Sect. 5 and some concluding remarks in Sect. 6.

## 2. Study area and input data

### 2.1. Mississippi River Basin

As case study area, the Mississippi River Basin (MRB) is defined. Covering an area of about  $3,000,000 \text{ km}^2$ , the MRB is the largest basin in North America and encompasses about 40% of the area of the United States. Moreover, it is the third largest in the world after Amazon and Congo basin [10]. It is a region that is densely populated. Already in 1982, 18 million people rely on the Mississippi for water supply [11]. This results in an intense anthropogenic water use, for which many large reservoirs have been build up. The Mississippi with its tributary Missouri is the longest (about  $3730 \text{ km}$ ) and largest (about  $16800 \text{ m}^3/\text{s}$ ) river in North America.

According to the WaterGAP hydrology model (see Sect. 2.5), a total number of 127 lakes and reservoirs are located in the MRB, from which only nine are defined as lakes and one as regulated lake. All others are reservoirs. Total water volume variations of  $180 \text{ km}^3$  and a surface area of  $14918 \text{ km}^2$  are documented for all water bodies (without rivers). The surface area varies between 3 and  $1127 \text{ km}^2$  and the storage changes up to  $18 \text{ km}^3$ . According to the Global Reservoir and Dam Database (GRanD) [12], a total water volume of about  $250 \text{ km}^3$  is stored in the reservoirs of MRB. The entire study area is shown in Fig. 1

### 2.2. Satellite altimetry data

Satellite altimetry determines the distance between the satellite and the Earth's surface in nadir direction by measuring the travel time of a microwave signal emitted by the instrument on board of the satellite and reflected by the water surface on ground. When the satellite's height is known, the surface elevation can be easily derived by subtracting both quantities [13]. Due to this measurement geometry, satellite altimetry provides measurements along dedicated profiles, i.e. tracks, with high along-track resolution (depending on sensor and datasets between about 300 m and 7 km). The cross-track resolution strongly depends on the satellite's orbit configuration. Most altimetry missions uses repeat orbits and cover the same location on Earth every 10 to 35 days. The higher the temporal resolution, the lower the spatial cross-track resolution. By combining different missions to a multi-mission approach, the temporal as well as the spatial resolution of the system can be significantly improved. In this study, six different orbits are exploited, which are used by more than ten different satellites. These are described in more detail in the following. Table 1 summarizes the orbit parameters for all these altimetry missions.



**Figure 1.** The Mississippi River Basin: Lakes and reservoirs that are implemented in WaterGAP are shown in blue, major rivers as grey lines. Orange: River sections that were removed manually (see Sect. 3.3).

The lifetime of satellite missions is limited to some years. In order to ensure a continuous and consistent monitoring of the Earth surface, successor missions follow the original ones on the same orbit. One important example for this, are the NASA/CNES missions TOPEX/Poseidon, Jason-1, Jason-2, and Jason-3 that will soon be continued by Sentinel-6. All these missions use the same nominal orbit with a repeat cycle of about 10 days and a track separation at the equator of about 315 km.

The second long-term orbit is occupied by ERS-1, ERS-2, and Envisat. These ESA missions are followed by the ISRO/CNES-mission Saral that uses the same orbit, but a different altimeter instrument operating in Ka-band; in contrast all other missions are emitting Ku-band signals. This orbit is defined as a 35-day repeat orbit with a 80-km track separation. Saral was launched in 2016, about three years after Envisat left his nominal orbit. During this data gap between Envisat and Saral, no measurements for this orbit had been acquired.

The Copernicus mission Sentinel-3 consists of two satellites: Sentinel-3A and Sentinel-3B. Both have the same orbit parameters but fly interleaved to each other with a 27-day repeat cycle each, so that they complement each other in spatial resolution. The Sentinel-3 constellation has a ground track separation at the equator of 52 km.

In addition to these short-repeat missions, two missions are used within this study flying on long- or non-repeat orbit. Cryosat-2 has a 369-day repeat. This results in a dense ground track pattern but in a sparse temporal resolution at dedicated locations. However, due to its sub-cycle of about 30 days, larger lakes can be monitored with monthly resolution.

Saral was originally using the Envisat orbit. However, due to problems with the satellite, since 2016, the orbit is no longer maintained on its nominal track but it's in a drifting configuration without long-term regular pattern in ground track. This results in an irregular spatial-temporal sampling on ground but can help monitoring lakes on a global scale, especially when this mission is combined with other altimetry missions. This part of the missions is named Saral-DP (drifting phase).

**Table 1.** Orbit configuration of satellite altimetry missions used in this study.

Orbit	missions	period	height [km]	repeat cycle [days]	track dist. at equator [km]
Jason	TOPEX, Jason-1/2/3	1992-today	1336	9.9	315
Envisat	ERS-1/2, Envisat, Saral	1991-2010/2013-2016	800	35	80
Sentinel-3A	Sentinel-3A	2016-today	815	27	104
Sentinel-3B	Sentinel-3B	2018-today	815	27	104
Cryosat-2	Cryosat-2	2010-today	717	369	8
Saral-DP	Saral-DP	2016-today	changing	drifting	irregular

### 2.3. Water occurrence masks

Water occurrence or probability masks are available from different sources. In this study we use the Global Surface Water dataset (GSW) published by Pekel *et al.* [14], as this has a global coverage and a high spatial resolution of about 30 m. It has been derived based on about three million Landsat satellite images taken between 1984 and 2015. For each pixel, the water probability given in percentage is provided, where a value of 50% might indicate either a permanent water occurrence of half of the pixel for all 32 years of data or a full water pixel for half of the time period. These values can be used to extract water masks for predefined water probability values, e.g. to derive lake shapes for permanent water bodies at dry seasons (threshold of 100%) or for areas temporarily flooded (threshold < 50%). More information on the methods used to convert GSW to land-water masks is provided in Sect. 3.1.

### 2.4. Global Lakes and Wetlands Database

For comparisons, information provided by the Global Lakes and Wetlands Database (GLWD) [15] is used in this study. Namely, shorelines and surface areas of Level 1 and Level 2. Level 1 provides metadata for the largest lakes (surface area  $\geq 50 \text{ km}^2$ ) and reservoirs (storage capacity  $\geq 0.5 \text{ km}^3$ ) worldwide. Level 2 contains additional smaller lakes with surface areas  $\geq 0.1 \text{ km}^2$ . For the MRB, the database provides 120 level 1 lakes and 4527 in level 2, with a total area of  $33,687.66 \text{ km}^2$  ( $19,041.73 \text{ km}^2$  for level 1 and  $14,645.83 \text{ km}^2$  for level 2).

### 2.5. Water volumes from WaterGAP

In order to analyse the surface water volume that can be monitored by satellite altimetry in the MRB, the WaterGap Global Hydrology Model WGHM [2] is used. The model is simulating water resources with a focus on anthropogenic interventions due to human water use and man-made reservoirs [16]. WGHM is using a spatial resolution of  $0.5^\circ$  and the temporal resolution of the model output used within this paper is monthly. A comprehensive description of the current model version 2.2d, which is used within the context of this study, is given by Müller Schmied *et al.* [16].

Water bodies are represented within the model as area fractions of the  $0.5^\circ$  grid cells. The GLWD (Sect. 2.4) and the GRanD database [12,17] are used for the definition of water bodies within the model. Each water body is defined as lake, regulated lake, reservoir or wetland. Furthermore, the model distinguishes between local and global water bodies: Lakes are implemented as global if their area is larger than  $100 \text{ km}^2$ , and for regulated lakes and reservoirs a threshold of  $0.5 \text{ km}^3$  storage capacity or  $100 \text{ km}^2$  minimum area is applied [16]. In this study, global lakes, regulated lakes and reservoirs are used (no local water bodies). As bathymetry and initial volume of the water bodies are unknown to the model, the WGHM water volumes for global water bodies are treated as anomalies. For reservoirs and regulated lakes, the maximum storage capacity is applied as an upper threshold [16]. The commissioning year (GranD database) is used to start filling reservoirs and if applicable changing the type of the water body from lake to regulated lake [16].

### 3. Method: Automated target detection

The identification of lakes and reservoirs that can be monitored by satellite altimetry needs information on the satellite's ground track on the one hand and knowledge of location and extent of water bodies on the other hand. The latter can be taken from existing data sets such as GLWD or Hydrosheds [18]. These provide constant water body shapes without considering any time-dependent variation due to seasonal or long-term changes. Alternatively, satellite images can be used to derive time-variable land-water or water occurrence masks, as for example available from optical Landsat and Sentinel-2 images [19]. Those data had already been used to derive inventories of global lakes, e.g. by Verpoorter *et al.* [20] and Feng *et al.* [21].

In this study, the Global Surface Water dataset (GSW) from Pekel *et al.* [14] (see Sect. 2.3) is used as input data. However, the developed procedure is able to handle any arbitrary water occurrence map in raster format, e.g. DAHITI occurrence masks [8]. Furthermore, it needs minimal manual interaction and is therefore suitable for large amounts of data, e.g. the MRB, and can be rerun easily if an updated version of the input water occurrence maps is available. The possibility to set parameters according to particular needs enables its application in variable scenarios; studies of water bodies with permanent water coverage or those that are only seasonally flooded.

The main idea is to identify connected water areas and to define the water body outlines based on a pre-defined threshold of water probability, which can later be transferred to other probability levels. The assumption is that all areas of one water body do have the same height. Thus, the approach is suitable for lakes and reservoirs but not for rivers. Due to the slope of the river, each satellite's overflight defines a new target (i.e. virtual station) at the crossing between the satellite's groundtrack and the river. For that reason, the developed approach is only applicable to lakes and reservoirs.

The developed algorithm consists of two major steps. First, individual water bodies are identified and labelled by applying several morphological operations that are widely used in image processing [22]. This is described in more detail in Sect. 3.1. In the second step (described in Sect. 3.2), isolated occurrence masks based on the GSW data are processed for each identified water body to analyse their coverage by satellite altimetry data at different water occurrence thresholds.

#### 3.1. Morphological operations and labelling

The basis for deriving the water masks is the GSW dataset introduced in Sect. 2.3. This is transformed into one binary land-water mask by defining a threshold value of 50%. This value will ensure the extraction of a mean surface area for permanent lakes/reservoirs with seasonal changing areas. Moreover, targets that are only temporally flooded will also be detected as well as reservoirs, which are created within the observation period of GSW, i.e. after 1984 but before about 2000. Later, masks for different water occurrences are derived (Sect. 3.2) and their impact is studied in Sect. 5.2.

The binary input mask is subject to three different morphological operations from image processing: erosion, dilation, and closing [22]. As structuring elements quadratic kernels are used. First, an **erosion** is performed on the binary input mask. This is done to remove small scale water bodies such as rivers, ponds, and very small lakes. For these small scale waters it is unlikely to infer satellite altimetry water level time series with sufficient data quality because of the influence of land (see Sect. 5.4). On the other hand, their removal speeds up the processing significantly. The kernel diameter is set to 21 pixels (approximately 630 m, depending on the geographic latitude), leading to a removal of all water bodies that are consistently narrower. The effect of this step is shown in Fig. 2: while subplot a displays the original binary mask, subplot b shows the resulting mask after the erosion was performed. Subsequently, the inverse operation called **dilation** is performed with a kernel size of approx. 4830 m (161 pixels), indicated by the grey area in Fig. 2c. In order to preserve original water body outlines, the result is overlain with the initial binary mask. Only pixels that are marked as water in both masks will be regarded as water in the resulting land water mask, i.e. the intersection between both is taken. This intersection is marked in white in Fig. 2c. In a last step, the **closing** operation with

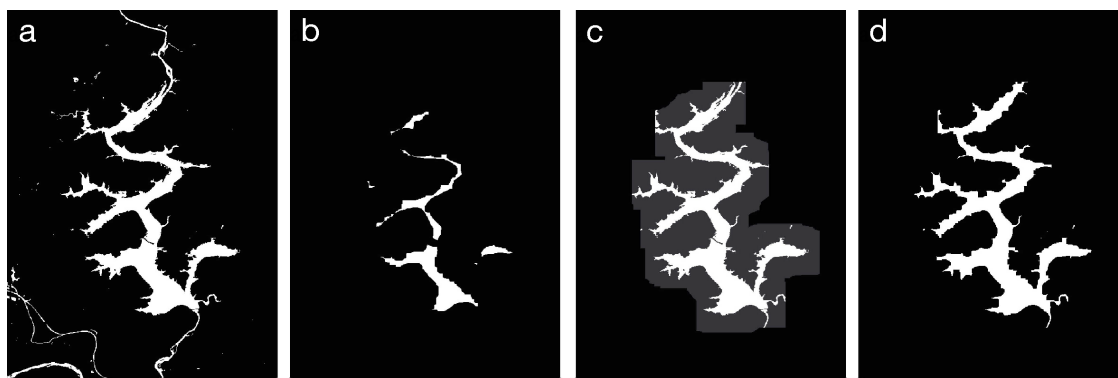


**Figure 2.** Visualization of the morphological operations used in the automated target detection: a) initial land-water mask, b) after erosion, c) after dilation, d) final land-water mask.

a kernel size of about 390 m (13 pixel) is applied. This operation removes small islands and bridges. This allows to unite two parts of a water body that are cut into two parts by e.g. bridges, cf. Fig. 2d.

This final land-water mask is submitted to the next processing step, namely the labelling algorithm to identify individual water bodies. An individual water body is defined as a set of connected pixels, i.e. pixels that share one edge. From this, a list of well-defined water bodies can be derived.

### 3.2. Lake shapes for different water occurrences

The target detection is performed based on a fixed water occurrence threshold of 50% (see Sect. 3.1). In order to conduct overflight statistics (Sect. 3.4) and to study the impact of different thresholds (Sect. 5.2), isolated water occurrence masks are required. Performing the morphological operations repeatedly for different thresholds (i.e. repeat the full image processing) is calculation and time demanding. Instead, the binary land-water mask (output of Sect. 3.1) covering the entire MRB is vectorized to reduce the computational time necessary to process the raster data. The result is one polygon feature per isolated water body. In order to extract the isolated water occurrence, the water occurrence mask is clipped to the bounding box of each feature with a buffer of  $0.15^\circ$ , which is required because narrow ends of dendritic reservoirs may have been lost due to the morphological operations. The clipped water occurrence mask is again transformed to a binary land-water mask, but this time with a occurrence threshold of 5%. Afterwards, each binary mask is labelled and the label of the corresponding water body is identified using the pole of inaccessibility (POI) of the respective polygon, i.e. the spot furthest from the lakeshore [23]. The POI is very likely located above a pixel of high occurrence. We isolate the water occurrence of each target using the respectively labelled pixels as a mask.

Due to the morphological operations, contiguous water bodies may be separated, especially at the shore of dendritic reservoirs. This results in duplicate isolated water occurrence masks. In order to detect these duplicates, intersections between the shorelines of all isolated mask are searched and the smaller intersecting masks are removed.

Based on the isolated water occurrence masks, water extent and surface area of each target can be extracted for different occurrence thresholds. In this study, we used thresholds of 5%, 25%, 50%, 75%, and 95% in order to calculate the satellite altimetry overflight statistics (Sect. 3.4).

### 3.3. Removal of rivers and coastal data

The aim of the automated target detection is to identify lakes and reservoirs, for which a constant water level per observation epoch is assumed. Due to the slope of rivers, water level time series can be derived only for particular river sections and not for entire rivers. For the same reason, most satellite altimetry time series for river targets are based on one single mission, except the rare cases of crossing tracks above a river. In consequence, rivers can not be processed like lakes and reservoirs, for which

the water level is assumed to be independent of the topography. Therefore, rivers are not part of this study and should not be part of the water targets detected.

Since rivers are part of GSW - and also of any other water occurrence product based on satellite images - they have to be excluded from the water mask within the process of target detection. This is easy for smaller rivers, which are removed by the erosional step. However, some rivers might be wider than some narrow reservoirs resulting from river impoundments. Therefore, it is not possible to define a kernel size that removes all rivers but preserves all lakes and reservoirs at the same time. Thus, all major rivers are removed manually from the binary dataset (resulting from Sect. 3.1) by setting all water pixels within the river polygons to land. All rivers sections removed manually from the binary dataset are indicated in orange in Fig. 1.

However, there are still remaining river segments in the isolated water occurrence masks caused by small water bodies nearby and partly connected to a river. These masks have to be manually identified and removed from the dataset as well as large connected water systems at the coast which can not clearly be defined as a single water body or distinguished from the ocean. The primary reason for the manual interaction is to provide reliable statistics for this paper. Significantly less interaction is required for the target detection itself.

### 3.4. Connection to satellite altimetry data

In order to decide whether a lake is mapped by one of the satellite altimetry missions, their ground tracks have to be analysed. For this purpose, the individual measurement locations instead of the nominal ground tracks are used. Thus, for each individual altimetry observation it is checked whether it is taken above one of the detected water bodies. With this strategy, also missions on non-repeat orbits such as Saral-DP can be handled.

A water body is regarded as monitored by a mission if at least four valid overflights per year (in average) are detected. This ensures the monitoring of the lake's seasonality even for missions on long- or non-repeat orbits (Cryosat-2 and Saral-DP). For the short-repeat missions (Envisat, Jason, and Sentinel-3A/B), which cover the same location every 10 to 35 days, the temporal resolution will be always better: at least once per month.

## 4. Results

The automated target detection approach described in Sect. 3 with a water occurrence threshold of 50% identifies 4535 water bodies with surface areas of 0.1 to 1,291.04 km<sup>2</sup> and a total sum of 29,100.72 km<sup>2</sup>. The mean area is 6.4 km<sup>2</sup>. 2061 lakes/reservoirs are larger than 1 km<sup>2</sup>, 429 larger than 10 km<sup>2</sup>, and 45 larger than 100 km<sup>2</sup>. While the number of detected water bodies is very close to the number given in GLWD (Level 1 and Level 2), which is 4647, the total area is underestimated by almost 4600 km<sup>2</sup> (GLWD area is 33,688 km<sup>2</sup>). This changes with different water occurrence adopted (see Sect. 3.2 for details). The number of water bodies as well as their surface area is increasing if no limitation of water occurrence is used (>5%). In this case, 5708 lakes large than 0.1 km<sup>2</sup> are identified with a total surface area of 35,397.54 km<sup>2</sup>. Figure 3 shows the numbers for different threshold of water occurrence probabilities. The blue line represents the results for all water bodies larger than 0.1 km<sup>2</sup>. For the red and orange lines larger lake size limits of 1 and 10 km<sup>2</sup> are applied. Number and size of detected lakes larger than 10 km<sup>2</sup> for higher water occurrences correspond well with those from GLWD Level 1 and WGHM.

### 4.1. Water bodies monitored by different altimetry configurations

Due to the profiled measurement geometry of satellite altimetry, not all detected water bodies can be monitored by that techniques. Depending on the orbit configuration (see Sect. 2.2) multiple lakes will be missed by some missions, especially smaller lakes.

Since the altimetry mission configuration is changing over time, four different scenarios have been defined and investigated regarding their lake coverage:

- 1. Jason only
- 2. Sentinel-3 only (both satellites)
- 3. Jason & Envisat (past configuration)
- 4. Jason & Sentinel-3 & Cryosat-2 & Saral-DP (current configuration)

The statistics presented here is based on a water occurrence of 50% and captures all water bodies larger than  $0.1\text{ km}^2$  (blue dot with black edge in Fig. 3). 3437 targets (75.7%) are not covered by any of the current and past missions under investigation. Since these are mostly smaller lakes or reservoirs, the percentage of not covered water area is only 17.5% (5108 out of  $29101\text{ km}^2$ ). Depending on the groundtracks of the different missions, they cover a different number of targets. The best scenario is the current configuration of Jason-3, Sentinel-3A/B, Cryosat, and Saral-DP that captures about 19% of the water bodies and 79% of the surface areas. With respect to past altimetry configurations (i.e. Jason-2 and Envisat) this is a significant improvement. All numbers are summarized in Tab. 2.

**Table 2.** Number and area of lakes/reservoirs larger than  $0.1\text{ km}^2$  covered by different altimetry constellations. The values in parentheses are the percentages of total number and total area, respectively.

Scenario	number of targets	area of targets in $\text{km}^2$	mean size of targets in $\text{km}^2$
Jason only	212 (4.7%)	9125 (31.3%)	43.0
Sentinel-3A/B	704 (15.5%)	20893 (71.7%)	29.7
past configuration	612 (13.5%)	18090 (62.0%)	29.6
current configuration	853 (18.8%)	23110 (79.3%)	27.1

As expected, most of the larger lakes are captured by the altimetry missions. The smaller a lake, the higher the probability that it is missed by the satellites. Fig. 4 shows the percentage of missed water bodies for the four different mission scenarios depending on the size of the lakes. With the current configuration, all lakes larger than  $50\text{ km}^2$  and almost 20% of the lakes larger than  $10\text{ km}^2$  are captured. This is a significant improvement with respect to the past configuration of Jason and Envisat, which misses almost 40% of all water bodies larger than  $20\text{ km}^2$ . However, even today, about 67% of all water bodies larger than  $1\text{ km}^2$  are missed in the MRB. This number will only be improved significantly, when a wide-swath altimetry mission such as SWOT planned for 2021 (see Sect. 5.5) will become

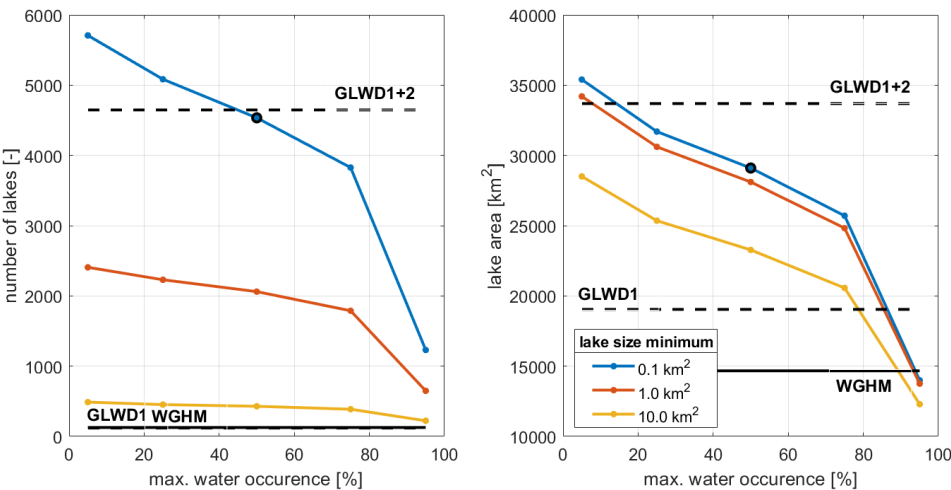


**Figure 3.** Number (left) and total area (right) of detected lakes in the MRB in dependence of adopted water occurrence for three different minimum lake sizes (blue:  $<0.1\text{ km}^2$ ; red:  $<1\text{ km}^2$ ; orange:  $<10\text{ km}^2$ ). The blue dots with black edge indicates the results for 50% water occurrence and  $0.1\text{ km}^2$  lake size limit, which are given in the text. Dashed black lines show number and area of GLWD (lower line: GLWD Level 1 only; upper line: GLWD Level 1+2). Solid black lines indicate numbers from WGHM.

active. When only using Jason, even more than 60% of lakes larger than  $100 \text{ km}^2$  can not be monitored, whereas the Sentinel-3 configuration alone performs already better than the past configuration of Jason and Envisat.

#### 4.2. Surface water storage

For the monitoring of the surface freshwater resources, water storage and its changes is more important than the number of lakes or their surface area. However, optical images as used in Sect. 3 are not able to provide any information on water volume or lake bathymetry. First approaches exist to derive storage changes and lake bathymetry from remote sensing techniques (as for example Schwatke *et al.* [8] and Li *et al.* [24]), also on a global scale [7],[25]. But since these approaches also rely on satellite altimetry, they are not able to provide information for all water bodies. The most comprehensive database for water volume are still global hydrological models, even if also in these records the very small water bodies are missing.

WGHM provides 127 lakes and reservoirs in the MRB with areas between  $2.9$  and  $1126.8 \text{ km}^2$  (total sum of  $14671.2 \text{ km}^2$ ) and water volume variations up to  $18.2 \text{ km}^3$ . From these targets, three reservoirs are not detected by the automated target detection developed in this study. They have a total area of about  $20 \text{ km}^2$  ( $2.9$ ,  $12.4$  and  $4.8 \text{ km}^2$ ) and are all very narrow. 125 of all detected targets are available in WGHM (2.8%) representing about 51% of the total detected surface area.

From the 127 WGHM targets, 116 can be mapped by one of the altimetry missions handled in this study, however, not at the same time. 11 are not covered at all. In the past, with a combination of satellites from the Jason and Envisat family (past configuration), about 76% of the water volume variations as issued by WGHM were detectable. In comparison, the current configuration of Jason, Sentinel-3, Cryosat-2, and Saral-DP meets the requirement to monitor 98% of the water volume of lakes and reservoirs in the MRB (since 2018). When using only Jason, this number is with about 50% much smaller. All numbers can be found in Tab. 3.

Although WGHM represents less than half of the available water surface area in the MRB, still about  $300 \text{ km}^2$  (2% of the WGHM total area) can not be mapped by satellite altimetry due to the orbit configuration of the missions. The averaged surface area of WGHM targets is  $116 \text{ km}^2$ , the mean size of mapped water bodies is  $124 \text{ km}^2$ . The percentage of missed water volume changes is in the same order of magnitude: about 2% of WGHM storage changes can not be monitored by today's satellite altimetry. Thus, it is reasonable to say that the current altimetry configuration is able to provide almost the same information than available from global hydrological models. However, the temporal resolution differs: while WGHM provides monthly values, the altimetry resolution can yield values from a few days to

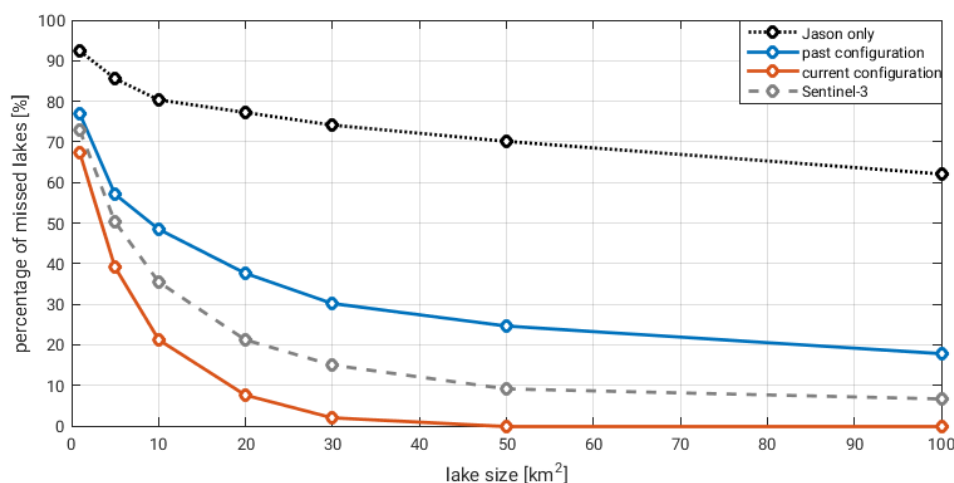


**Figure 4.** Percentage of missed lakes/reservoirs for different altimetry configurations depending on minimal target size (from 1 to  $100 \text{ km}^2$ ) based on an water occurrence threshold of 50%.

**Table 3.** Water storage changes from WGHM that are mapped by different altimetry constellations. The values in parentheses are the percentages of total number and total volume variations from WGHM, respectively.

Scenario	number of targets	water volume variation in $km^3$	mean variations in $km^3$	mean size in $km^2$
Jason only	29 (22.8%)	90.6 (50.4%)	3.13	224.2
Sentinel-3A/B	97 (76.4%)	161.9 (90.1%)	1.67	129.7
past configuration	71 (55.9%)	137.1 (76.3%)	1.93	158.5
current configuration	116 (91.3%)	176.5 (98.1%)	1.52	123.9

10 or 35 days or even worth, depending on the missions involved (see Sect. 2.2 and 5.4). However, when it is about long-term storage changes approximately 25% are missed by the satellites, even 50% when only Jason missions are used. These numbers improve when only looking at larger lakes (see Fig. 5). With the current configuration storage changes of all lakes larger than  $80 km^2$  can be monitored, whereas Jason still misses about  $15 km^3$  for lakes larger than  $200 km^2$ .

It should be noted that all numbers presented here are based on information about the satellites' orbit configuration, i.e. whether a lake is or is not crossed by any of the satellites' tracks. Additional lakes will be missed when no reliable height information can be determined, which is especially conceivable for small lakes with steep surrounding topography (see Sect. 5.4 for more details).

## 5. Discussion

### 5.1. Assessment of automated target detection

With 5708 targets, there are about 1000 water bodies more identified in this study (applying an occurrence threshold of 5%) compared to the 4647 given by GLWD Level 1 and 2 data (cf. Fig. 3). However, the datasets not only differ by additional water bodies identified in this study, but also by some missing targets which are contained in GLWD.

As example, Fig. 6 shows an area along the Red River at the border between Arkansas and Oklahoma. Several water bodies identified in this study are not part of the GLWD Level 1 or 2, such as the lakes Jim Chapman, McGee Creek, Hinkle, and some smaller targets east of the Jim Chapman Lake, which itself is contained in WGHM, though. However, some water bodies are not identified, even though available in GLWD. Either, like Lake Gillham, they are too small, i.e. consistently narrower than

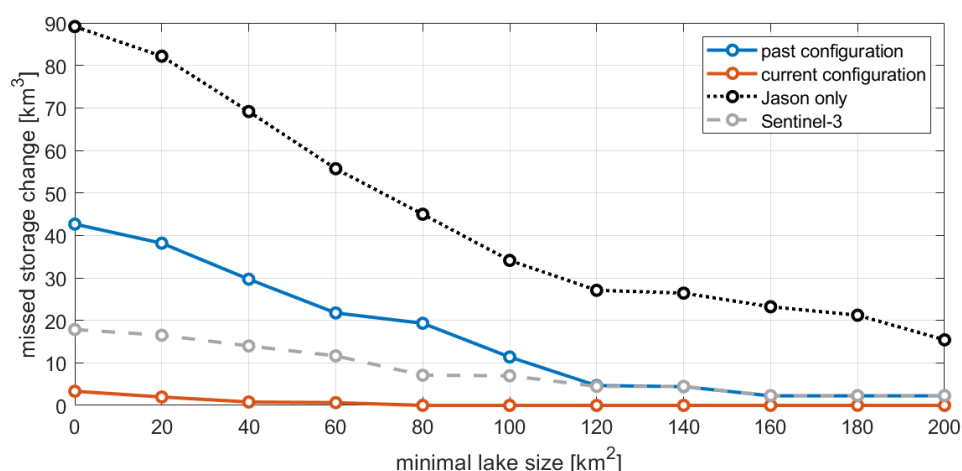


**Figure 5.** Missed WGHM storage changes as function of minimal lake size for different altimetry configurations.

630 m, and removed by the morphological operations (Sect. 3.1), or they are connected to a river (by water occurrence pixels above 5%) and removed manually (Sec. 3.3) as they could not be distinguished from the river. Also noteworthy is the different size of some lakes. For example, Lake Hugo and Lake Wister, are both much smaller in GLWD than in this study.

Sometimes, the separation between lake and river is not clear, since the method is not able to distinguish between a narrow reservoir and a wide river. In these cases, part of the river is identified as lake area (e.g. Lake Broken Bow and Millwood Lake). In rare cases, such targets can cause an error in the overflight statistics when the satellite track crosses the connected remaining river but not the water body which is the actual target. On a basin-wide average the water surface area differs by 1710  $\text{km}^2$  (about 5%) with respect to GLWD, see Fig. 3.

Other challenges arise due to the definition of targets. A good example are Lake Barkley and Kentucky shown in Fig. 7 which are actually one water body connected by the unregulated Barkley Canal. While they are automatically identified as one target in this study, as indicated by the green polygon in Fig. 7, they are treated separately in the GLWD dataset. Another challenge in terms of definition is the extent of an reservoir upstream of the respective dam. There is no clear border between the river and the reservoir and thus the size of both lakes is larger in GLWD compared to this study.

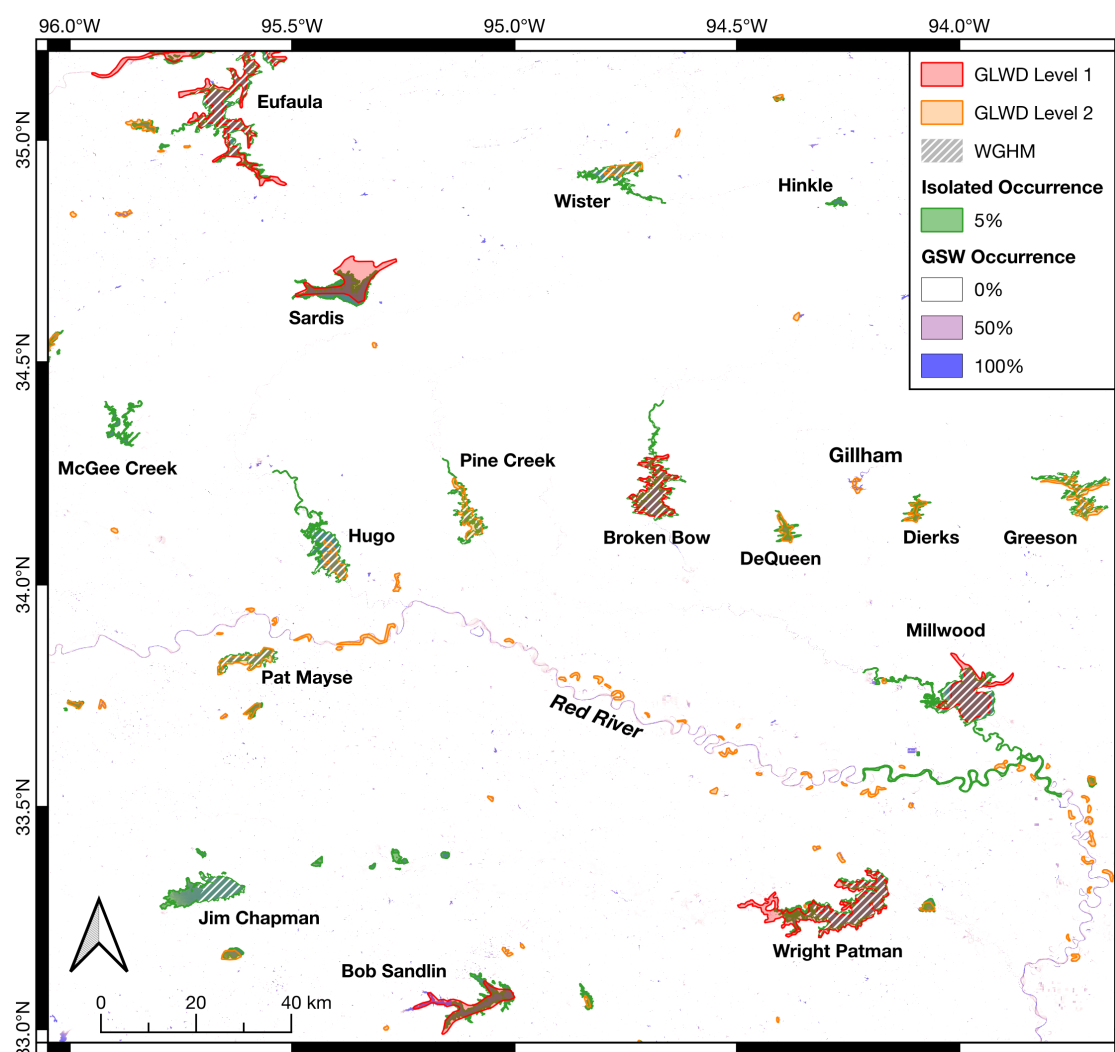


**Figure 6.** Isolated occurrence of detected targets (green), GLWD Level 1 (red) and 2 (orange), and WGHM data (white hatched) surrounding the Red River at the border between Arkansas and Oklahoma. Additionally the GSW water occurrence is shown as background.

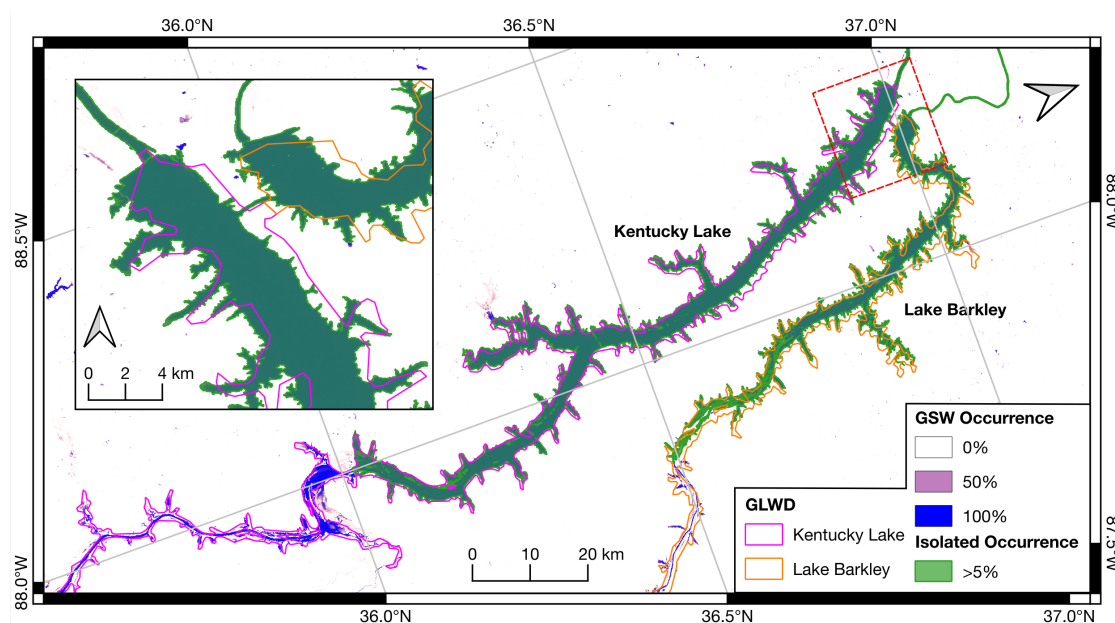


**Figure 7.** Lake Barkley and Kentucky, separated in the GLWD data (purple and orange) and merged in the isolated results of this study (green). Additionally the GSW water occurrence is shown as background. The inset shows the area close to the dams and the Barkley Canal connecting both lakes.

The comparison also shows that the water body outline identified in this study is more detailed and accurate than the GLWD data.

Challenging conditions are also found at the coastal wetlands where some possible targets can not be distinguished from the ocean or connected water bodies. In rare cases, targets are removed by the erosional step or the POI is not within the area of high occurrence of a water body (e.g. an island) resulting in an incorrect label and isolation. Both errors occur predominantly at narrow dendritic reservoirs.

By changing the pixel sizes of the morphological operation, the method can be optimized to find more or less narrow structures. However, automated processes will never be able to distinguish a bridge over a reservoir (that should be removed from the images) from a same-sized dam of a reservoir (that should be left in the image). The applied parameters have proved to be a good compromise to detect most of the relevant water bodies without identifying too much unwanted targets. However, since no ground truth is available, a fine-tuning based on statistical validation for the entire MRB is not possible.

## 5.2. Impact of different water occurrences

The overflight statistics presented in Sect. 4.1 will change with varying lake's shape: At high water level the lake will cover a larger area and will be crossed by an altimeter track with higher probability. In this study, occurrence masks are used to extract lake shapes for different water levels (Sect. 3.2). When increasing the water occurrence threshold from 50% to 95% the number of detected lakes is decreasing (see Fig. 3), since only permanent water is counted. At the same time, the mean size of the detected lakes increases (from 6.4 to 11.4 km<sup>2</sup>) as more larger lakes have permanent flooded parts. Consequently, less lakes are missed by the altimetry missions when the occurrence threshold is increased. Instead, with decreasing occurrence threshold more lakes can not be monitored since they are no longer crossed by a satellite's track. Figure 8 illustrates the percentage of missed lakes for different water occurrences for lakes larger 0.1 km<sup>2</sup> and lakes larger than 10 km<sup>2</sup>. Whereas nearly 90% of the smaller non-permanent lakes are missed by the past altimetry configuration (and still 85% by the current one), these numbers decrease to 75% and 63%, respectively. When limiting the analysis to

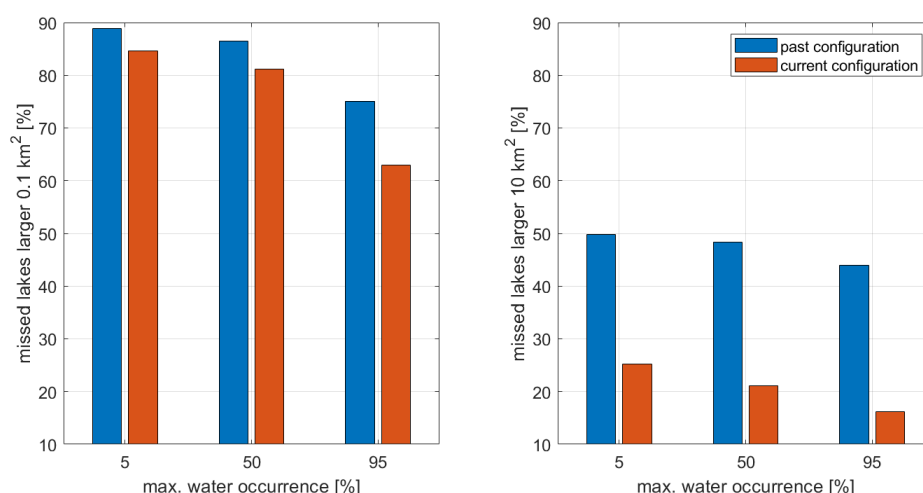


**Figure 8.** Percentage of missed lakes/reservoirs for different altimetry configurations and different water occurrences. Left: all water bodies larger than 0.1 km<sup>2</sup>; right: water bodies larger than 10 km<sup>2</sup>.

lakes larger than 10 km<sup>2</sup>, the number of missed lakes is smaller for all occurrence threshold but shows the same behaviour. The current configuration of altimetry satellites is able to monitoring about 84% of these lakes when taking all occurrences into account.

It may be worth mentioning that with decreasing water occurrence not only altimetry observations are less frequent but also lower quality due to increased land contamination is expected (see Sect. 5.4).

### 5.3. Impact of neglecting rivers and smaller lakes not available in WGHM

When investigating the percentage of monitored surface water storage in Sect. 4.2 smaller lakes that are not available in WGHM as well as water available in rivers have been neglected.

Rivers only store 0.006% of the global freshwater [26]. River water storage comprises less than 0.5% of the freshwater on Earth (without groundwater and water stored as ice), whereas lakes store nearly 21% [1]. The small percentage of river water justifies the focus on lakes and reservoirs. Even if the Mississippi contains more water than most other rivers, the entire MRB is so large that global conditions can be assumed.

The impact of neglecting lakes smaller than 0.1 km<sup>2</sup> can be assessed using analyses performed by Downing *et al.* [27] based on statistical extrapolations. They estimate the number of lakes with areas from 0.001 to 0.1 km<sup>2</sup> to be 99% of all lakes and covering about 30% of the overall global lake area. When assuming that this relation can be transferred to the MRB, 30% of the total lake area would have been missed due to the neglect of lakes smaller than 0.1 km<sup>2</sup>: 12472 km<sup>2</sup>. The lower percentage published by Verpoorter *et al.* [20] (about 4.8% of the area of all lakes leading to a neglect of around 2000 km<sup>2</sup>) based on remote sensing data is at least partly due to the spatial resolution and detection limit of the used satellite imagery. However, it documents well the still missing knowledge on the number and area of small lakes on Earth. Current remote sensing instruments are not able to set light on this since the spatial resolution of satellite techniques is limited. Moreover, the lake abundance is changing rapidly in some regions [20] and every study can only be a snapshot of the respective situation.

With respect to lake volume changes, the relation presented by Biancamaria *et al.* [28] suggests that 20% of the global storage changes are due to lakes smaller than 0.1 km<sup>2</sup>. Due to the resolution limits of satellite altimetry (including SWOT), these percentage can not be monitored from space in the foreseeable future. Assuming that WGHM includes all water bodies with areas larger about 3 km<sup>2</sup>, it should capture a bit more than 50% of storage changes. Consequently, nearly 50% (about 180 km<sup>3</sup>) are not included in WGHM. If one aims at smaller lakes, regional hydrological models must be used.

#### 5.4. Limitations in satellite altimetry height estimation

It is important to keep in mind, that even if a lake or reservoir is located beneath a groundtrack of a satellite altimetry mission, it is not always possible to derive valid height information. The ability for reliable generation of water level time series strongly depends on the size of a water body, especially on the length of the satellite's track over the water, but this is not the only influence. The quality of the measurements are also affected by the surrounding topography, the sensor type on board of the satellite and other factors. Thus, no generally applicable size limit can be defined. While Biancamaria *et al.* [28] states a limit of  $100 \text{ km}^2$  referencing to work from 2002 and 2006, Baup *et al.* [29] show results for a  $0.52 \text{ km}^2$  small lake in France, and Biancamaria *et al.* [30] use satellite altimetry for monitoring the River Garonne that is only 200 m wide.

For the MRB, using the DAHITI processing approach [31], reliable long-term water level time series for 54 lakes and reservoirs can be derived, from which 41 targets are part of WGHM. This is about 58% of the WGHM targets mapped by the past altimetry configuration. The minimal size of the observed WGHM lakes is  $10 \text{ km}^2$ . The smallest lake for which water level time series can be derived and which is not part of WGHM is  $3.4 \text{ km}^2$  (with 50% occurrence threshold). For the WGHM targets missing in DAHITI, no accurate long-term water level time series can be derived. This is mostly due to the shape of the lakes (very narrow) or due to satellite tracks close to the lakes' shorelines. However, it is important to keep in mind that these number are not easily transferable to other basins, since the local characteristics strongly influence the quality of altimetry-derived water level time series.

Another point worth to mention here is the temporal resolution of the altimetry-derived time series. As already indicated in Sect. 2.2, this strongly depends on the repeat cycle of the satellite as well as on the number of tracks covering a lake or reservoir. In this study, a water body is counted as monitored when at least four overflights per year are identified (see Sect. 3.4). Thus, time series with temporal resolutions of three months up to a few days can be generated, depending on the lakes size and location. This ensures to capture seasonal variations but will not guarantee the monitoring of short-time extreme events, especially for smaller lakes.

#### 5.5. Outlook to SWOT

The "Surface Water and Ocean Topography" mission SWOT is planned to be launched in 2021. In addition to a classical nadir-looking Ku-band altimeter, the mission will carry a Ka-band radar interferometer called KaRin. This instrument will provide water level height information in two 50 km wide swaths with a 20 km nadir gap (that is partly covered by the nadir altimeter) [32]. The spatial resolution within this 120 km wide area varies between 10 and 60 m with an along-track pixel size of 2.5 m [32]. Consequently, SWOT will cover nearly all continental surfaces up to a latitude of  $\pm 78^\circ$  without larger data gaps. The total gap area in this region is about 3.5% of the total land area [33], mostly located close to the equator. For the MRB that is located north of  $25^\circ \text{N}$  no gaps due to the orbit configuration will occur, and all water bodies will be covered at least once within the 21 day repeat period. The temporal resolution strongly depends on the geographic latitude and will be differ between two and four times per 21 days within the MRB (unevenly distributed). This is still not optimal and will not lead to all extreme events being caught. However, the combination with observations from classical missions will further increase the temporal resolution of several time series.

Even if the requirement of SWOT is to monitor all lakes larger than  $1 \text{ km}^2$  [28], the mission aims to measure spatio-temporal variability of lakes and reservoirs larger than approximately 250 by 250 m or  $0.06 \text{ km}^2$  [34]. Thus, about two-thirds of global lake and reservoir storage variations can be captured [33]. Moreover, SWOT can also provide information on the surface area of lakes and reservoirs, thus, perform its own target detection. This also enables the determination of improved storage information from the simultaneously measured area and height information.

Thus, the future prospects are excellent thanks to SWOT. However, long-term studies still dependent on the older, incomplete data from classical missions. Moreover, careful calibration and

combination concepts are necessary in order to ensure a consistent linkage of SWOT with historical datasets and with data from current nadir altimeters.

## 6. Conclusions

Using the example of the Mississippi River Basin, this study shows the potential and limitations of satellite altimetry to monitor basin-wide surface water storage changes. Based on a newly developed automated target detection, the number and size of all lakes larger than about  $0.1 \text{ km}^2$  in the MRB can be determined. The merging of this information with past and current satellite altimeter constellations reveals an overview on the possibilities of remote sensing technique to monitor lake storage changes from space.

With the developed target detection approach, about 5700 lakes and reservoirs can be detected in the MRB. This is in accordance to the information of GLWD, even if a larger total surface area is documented there. The number reduces significantly, when only water bodies with permanent water are taken into account.

The study reveals, that in the MRB today, with the current altimeter configuration consisting of Jason, Sentinel-3, Cryosat-2, and Saral-DP, only about 20% of water bodies larger than  $0.1 \text{ km}^2$  can be captured by satellite altimetry. This number increases to about 80% for lakes larger than  $10 \text{ km}^2$ , even though not for all of them reliable water level time series are determinable. The main limitation is the measurement technique requiring the satellites to directly overpass the water bodies for reliable measurements. When analysing larger water bodies available in the global hydrology model WGHM, the situation improves: From these larger lakes more than 90% are captured by satellite altimetry and 98% of the related storage changes can be monitored. However, for long-term studies relying on past altimeter configurations the situation is significantly worse: until 2016, nearly 25% of storage changes (i.e. more than  $40 \text{ km}^3$ ) are missed by the satellite tracks.

This study is limited to the MRB and not directly transferable to other basins with different lake density and characteristics. However, since the region is quite large with significant variations in the number of lakes per  $10^6 \text{ km}^2$  [27], transferability to a global scale might be valid.

Significant improvements are expected by the new SWOT mission that will cover the entire MRB without any data gap due to the orbit configuration of the mission. Moreover, smaller lakes will be reliably measured due to the higher spatial resolution and an increase height precision. Thus, after 2021 the greatest limitation of satellite altimetry will be the temporal resolution of time series and the risk to miss extreme short-periodic events.

**Author Contributions:** D.D. conceptualized the research work and wrote the major part of the manuscript; L.E. developed the automated target detection and prepared a draft version of the paper. L.E., C.S and D.S. did the data processing. C.N. provided the lake volume changes from WGHM. C.S., D.S. and C.N. contributed to the manuscript writing and helped with the discussions of the applied methods and results. All authors have read and agreed to the published version of the manuscript.

**Funding:** This research was funded by the German Research Foundation DFG grant number DE 2174/10-1.

**Acknowledgments:** The authors would like to acknowledge the European Commission's Joint Research Centre for allowing access to the Global Surface Water Explorer GSWE (<https://global-surface-water.appspot.com/>). The support of the German Research Foundation (DFG) within the framework of the Research Unit GlobalCDA (FOR2630) is gratefully acknowledged.

**Conflicts of Interest:** The authors declare no conflict of interest.

## References

1. Shiklomanov, I. World fresh water resources. In *Water in Crisis: A Guide to the World's Fresh Water Resources*; Gleick, P., Ed.; Oxford University Press, 1993; pp. 13–23.
2. Müller Schmied, H.; Eisner, S.; Franz, D.; Wattenbach, M.; Portmann, F.T.; Flörke, M.; Döll, P. Sensitivity of simulated global-scale freshwater fluxes and storages to input data, hydrological model

- structure, human water use and calibration. *Hydrology and Earth System Sciences* **2014**, *18*, 3511–3538. doi:10.5194/hess-18-3511-2014.
3. Döll, P.; Douville, H.; Güntner, A.; Müller Schmied, H.; Wada, Y. Modelling Freshwater Resources at the Global Scale: Challenges and Prospects. *Surveys in Geophysics* **2016**, *37*, 195–221. doi:10.1007/s10712-015-9343-1.
4. Alsdorf, D.E.; Rodríguez, E.; Lettenmaier, D.P. Measuring surface water from space. *Reviews of Geophysics* **2007**, *45*. doi:10.1029/2006rg000197.
5. Zaitchik, B.F.; Rodell, M.; Reichle, R.H. Assimilation of GRACE Terrestrial Water Storage Data into a Land Surface Model: Results for the Mississippi River Basin. *Journal of Hydrometeorology* **2008**, *9*, 535–548. doi:10.1175/2007JHM951.1.
6. Gao, H. Satellite remote sensing of large lakes and reservoirs: from elevation and area to storage. *WIREs Water* **2015**, *2*, 147–157. doi:10.1002/wat2.1065.
7. Busker, T.; de Roo, A.; Gelati, E.; Schwatke, C.; Adamovic, M.; Bisselink, B.; Pekel, J.F.; Cottam, A. A global lake and reservoir volume analysis using a surface water dataset and satellite altimetry. *Hydrology and Earth System Sciences* **2019**, *23*, 669–690. doi:10.5194/hess-23-669-2019.
8. Schwatke, C.; Dettmering, D.; Seitz, F. Volume Variations of Small Inland Water Bodies from a Combination of Satellite Altimetry and Optical Imagery. *Remote Sensing* **2020**, *12*. doi:10.3390/rs12101606.
9. Durand, M.; Fu, L.L.; Lettenmaier, D.P.; Alsdorf, D.E.; Rodriguez, E.; Esteban-Fernandez, D. The Surface Water and Ocean Topography Mission: Observing Terrestrial Surface Water and Oceanic Submesoscale Eddies. *Proceedings of the IEEE* **2010**, *98*, 766–779. doi:10.1109/jproc.2010.2043031.
10. Niebling, W.; Baker, J.; Kasuri, L.; Katz, S.; Smet, K. Challenge and response in the Mississippi River Basin. *Water Policy* **2014**, *16*, 87–116. doi:10.2166/wp.2014.005.
11. Mississippi River Facts. Online information at <https://www.nps.gov/miss/riverfacts.htm>. Last accessed on July 07, 2020.
12. Lehner, B.; Liermann, C.R.; Revenga, C.; Vörösmarty, C.; Fekete, B.; Crouzet, P.; Döll, P.; Endejan, M.; Frenken, K.; Magome, J.; Nilsson, C.; Robertson, J.C.; Rödel, R.; Sindorf, N.; Wissler, D. High-resolution mapping of the world's reservoirs and dams for sustainable river-flow management. *Frontiers in Ecology and the Environment* **2011**, *9*, 494–502. doi:10.1890/100125.
13. Chelton, D.; Ries, J.; Haines, B.; Fu, L.L.; Callahan, P., Satellite Altimetry and Earth Sciences. A Handbook of Techniques and Applications; Academic Press, 2001; chapter Satellite Altimetry.
14. Pekel, J.F.; Cottam, A.; Gorelick, N.; Belward, A.S. High-resolution mapping of global surface water and its long-term changes. *Nature* **2016**, *540*, 418–422. doi:10.1038/nature20584.
15. Lehner, B.; Döll, P. Development and validation of a global database of lakes, reservoirs and wetlands. *Journal of Hydrology* **2004**, *296*, 1–22. doi:10.1016/j.jhydrol.2004.03.028.
16. Müller Schmied, H.; Cáceres, D.; Eisner, S.; Flörke, M.; Herbert, C.; Niemann, C.; Peiris, T.A.; Popat, E.; Portmann, F.T.; Reinecke, R.; Schumacher, M.; Shadmok, S.; Telteu, C.E.; Trautmann, T.; Döll, P. The global water resources and use model WaterGAP v2.2d: Model description and evaluation. *Geoscientific Model Development Discussions* **2020**, *2020*, 1–69. doi:10.5194/gmd-2020-225.
17. Döll, P.; Fiedler, K.; Zhang, J. Global-scale analysis of river flow alterations due to water withdrawals and reservoirs. *Hydrology and Earth System Sciences* **2009**, *13*, 2413–2432. doi:10.5194/hess-13-2413-2009.
18. Lehner, B.; Verdin, K.; Jarvis, A. New Global Hydrography Derived From Spaceborne Elevation Data. *Eos, Transactions American Geophysical Union* **2008**, *89*, 93. doi:10.1029/2008EO100001.
19. Schwatke, C.; Scherer, D.; Dettmering, D. Automated Extraction of Consistent Time-Variable Water Surfaces of Lakes and Reservoirs Based on Landsat and Sentinel-2. *Remote Sensing* **2019**, *11*. doi:10.3390/rs11091010.
20. Verpoorter, C.; Kutser, T.; Seekell, D.A.; Tranvik, L.J. A global inventory of lakes based on high-resolution satellite imagery. *Geophysical Research Letters* **2014**, *41*, 6396–6402. doi:10.1002/2014GL060641.
21. Feng, M.; Sexton, J.O.; Channan, S.; Townshend, J.R. A global, high-resolution (30-m) inland water body dataset for 2000: first results of a topographic–spectral classification algorithm. *International Journal of Digital Earth* **2016**, *9*, 113–133. doi:10.1080/17538947.2015.1026420.
22. Bovik, A.C. Basic Binary Image Processing. In *The Essential Guide to Image Processing*; Elsevier, 2009; pp. 69–96. doi:10.1016/b978-0-12-374457-9.00004-4.
23. Garcia-Castellanos, D.; Lombardo, U. Poles of inaccessibility: A calculation algorithm for the remotest places on earth. *Scottish Geographical Journal* **2007**, *123*, 227–233. doi:10.1080/14702540801897809.

24. Li, Y.; Gao, H.; Zhao, G.; Tseng, K.H. A high-resolution bathymetry dataset for global reservoirs using multi-source satellite imagery and altimetry. *Remote Sensing of Environment* **2020**, *244*, 111831. doi:https://doi.org/10.1016/j.rse.2020.111831.
25. Tortini, R.; Noujdina, N.; Yeo, S.; Ricko, M.; Birkett, C.M.; Khandelwal, A.; Kumar, V.; Marlier, M.E.; Lettenmaier, D.P. Satellite-based remote sensing data set of global surface water storage change from 1992 to 2018. *Earth System Science Data* **2020**, *12*, 1141–1151. doi:10.5194/essd-12-1141-2020.
26. Gleick, P. Water resources. In *Encyclopedia of Climate and Weather*; Schneider, S., Ed.; Oxford University Press, 1996; pp. 817–823.
27. Downing, J.A.; Prairie, Y.T.; Cole, J.J.; Duarte, C.M.; Tranvik, L.J.; Striegl, R.G.; McDowell, W.H.; Kortelainen, P.; Caraco, N.F.; Melack, J.M.; Middelburg, J.J. The global abundance and size distribution of lakes, ponds, and impoundments. *Limnology and Oceanography* **2006**, *51*, 2388–2397. doi:10.4319/lo.2006.51.5.2388.
28. Biancamaria, S.; Andreadis, K.M.; Durand, M.; Clark, E.A.; Rodriguez, E.; Mognard, N.M.; Alsdorf, D.E.; Lettenmaier, D.P.; Oudin, Y. Preliminary Characterization of SWOT Hydrology Error Budget and Global Capabilities. *IEEE Journal of Selected Topics in Applied Earth Observations and Remote Sensing* **2010**, *3*, 6–19. doi:10.1109/jstars.2009.2034614.
29. Baup, F.; Frappart, F.; Maubant, J. Combining high-resolution satellite images and altimetry to estimate the volume of small lakes. *Hydrology and Earth System Sciences* **2014**, *18*, 2007–2020. doi:10.5194/hess-18-2007-2014.
30. Biancamaria, S.; Frappart, F.; Leleu, A.S.; Marieu, V.; Blumstein, D.; Desjonquères, J.D.; Boy, F.; Sottolichio, A.; Valle-Levinson, A. Satellite radar altimetry water elevations performance over a 200m wide river: Evaluation over the Garonne River. *Advances in Space Research* **2017**, *59*, 128 – 146. doi:10.1016/j.asr.2016.10.008.
31. Schwatke, C.; Dettmering, D.; Bosch, W.; Seitz, F. DAHITI – an innovative approach for estimating water level time series over inland waters using multi-mission satellite altimetry. *Hydrology and Earth System Sciences* **2015**, *19*, 4345–4364. doi:10.5194/hess-19-4345-2015.
32. Fjørtoft, R.; Gaudin, J.; Pourthié, N.; Lalaurie, J.; Mallet, A.; Nouvel, J.; Martinot-Lagarde, J.; Oriot, H.; Borderies, P.; Ruiz, C.; Daniel, S. KaRIn on SWOT: Characteristics of Near-Nadir Ka-Band Interferometric SAR Imagery. *IEEE Transactions on Geoscience and Remote Sensing* **2014**, *52*, 2172–2185. doi:10.1109/TGRS.2013.2258402.
33. Biancamaria, S.; Lettenmaier, D.P.; Pavelsky, T.M. The SWOT Mission and Its Capabilities for Land Hydrolog. *Surveys in Geophysics* **2016**, *37*, 307–337. doi:10.1007/s10712-015-9346-y.
34. Solander, K.C.; Reager, J.T.; Famiglietti, J.S. How well will the Surface Water and Ocean Topography (SWOT) mission observe global reservoirs? *Water Resources Research* **2016**, *52*, 2123–2140. doi:10.1002/2015WR017952.